Physical and Chemical Speciation of Iron in the Polar Oceans

Thuróczy, Charles-Edouard

Chapter 4

Observation of consistent trends in the organic complexation of dissolved iron in the Atlantic sector of the Southern Ocean

This chapter is adapted from: Thuróczy, C.-E., Gerringa, L.J.A., Klunder, M.B., Laan, P., De Baar, H.J.W., 2011a. Observation of consistent trends in the organic complexation of dissolved iron in the Atlantic sector of the Southern Ocean. Deep-Sea Research II. doi: 10.1016/j.dsr2.2011.01.002.

Abstract

Organic complexation of dissolved iron (DFe) was investigated in the Atlantic sector of the Southern Ocean in order to understand the distribution of Fe over the whole water column. The total concentration of dissolved organic ligands ([Lt]) measured by voltammetry ranged between 0.54 and 1.84 Eq of nM Fe whereas the conditional binding strength (K') ranged between $10^{21.4}$ and $10^{22.8}$. For the first time, trends in Fe-organic complexation were observed in an ocean basin by examining the ratio ([Lt]/[DFe]), defined as the organic ligand concentration divided by the dissolved Fe concentration. The [Lt]/[DFe] ratio indicates the saturation state of the natural ligands with Fe; a ratio near 1 means saturation of the ligands leading to precipitation of Fe. Reversely, high ratios mean Fe depletion and show a high potential for Fe solubilisation. In surface waters where phytoplankton is present low dissolved Fe and high variable ligand concentrations were found. Here the [Lt]/[DFe] ratio was on average 4.4. It was especially high (5.6-26.7) in the HNLC (High Nutrient, Low Chlorophyll) regions, where Fe was depleted. The [Lt]/[DFe] ratio decreased with depth due to increasing dissolved Fe concentrations and became constant below 450 m, indicating a steady state between ligand and Fe. Relatively low [Lt]/[DFe] ratios (between 1.1 and 2.7) existed in deep water north of the Southern Boundary, facilitating Fe precipitation. The [Lt]/[DFe] ratio increased southwards from the Southern Boundary on the Zero Meridian and from east to west in the Weddell Gyre due to changes both in ligand characteristics and in dissolved iron concentration. High [Lt]/[DFe] ratio expresses Fe depletion versus ligand production in the surface. The decrease with depth reflects the increase of [DFe] which favours scavenging and (co-) precipitation, whereas a horizontal increase in the deep waters results from an increasing distance from Fe sources. This increase in the [Lt]/[DFe] ratio at depth shows the very resistant nature of the dissolved organic ligands.

1. Introduction

The presence and availability of iron (Fe) is vital for life in the ocean. This trace nutrient is used by most organisms in seawater including phytoplankton in the euphotic zone. Phytoplankton is not only the base of the food web; it is also largely responsible for the fixation of dissolved carbon dioxide and the production of dissolved oxygen. Iron is used in phytoplankton cells in different locations and processes (Sunda *et al.* 1991 and 2001), notably in photosynthesis (photosystems) and in enzymes (*e.g.* nitrate-reductase). Due to its low concentration in seawater, iron is a limiting factor of primary production (Martin and Gordon, 1988, Martin *et al.*, 1991; De Baar *et al.*, 1990 and 1995; Buma *et al.*, 1991; Coale *et al.*, 1996; Fitzwater *et al.*, 1996; Timmermans *et al.*, 1998, 2001 and 2004), especially in HNLC (High Nutrient, Low Chlorophyll, Martin *et al.*, 1991) regions such as those in the Southern Ocean. Iron is used in the surface by phytoplankton but also over the whole water column by microbial communities (Bacteria and Archaea; Tortell *et al.*, 1996 and 1999) responsible for the degradation and remineralisation of sinking organic matter. Iron is found in seawater at concentrations above those determined by the solubility product (Kuma *et al.*, 1996; Millero, 1998). This is due to Fe binding organic ligands. Indeed 95 to 99.9 % of the dissolved Fe is strongly complexed by natural organic ligands (Gledhill and Van Den Berg, 1994; Rue and Bruland, 1995; Wu and Luther, 1995; Nolting *et al.*, 1998; Powell and Donat, 2001) allowing Fe to remain in solution, yet possibly limiting its availability for direct biological uptake.

The knowledge of the chemistry of Fe is important to understand its cycle in the world ocean which determines its distribution over the water column. The distribution of Fe in the oceans is controlled by its sources (aerosols deposition to the surface ocean, upwelling, ice melting and hydrothermal events), and by competition between processes which stabilise and remove it. Organic complexation stabilises Fe in seawater by keeping it in solution thus increasing its residence time. Fe removal is mainly caused by precipitation as oxy-hydroxides, adsorption onto large particles or colloid aggregation. (Alldredge *et al.*, 1993; Wells *et al.*, 1993, 1994 and 2000; Kepkay *et al.*, 1994; Logan *et al.*, 1995; Wu *et al.*, 2001; Cullen *et al.*, 2006).

The work presented here forms part of the GEOTRACES program (www.geotraces.org, Geotraces Science Plan, 2006). As part of this program, the

distribution of Fe along the Zero Meridian (Klunder *et al.*, 2011) and several other trace elements, including dissolved aluminium and manganese (Middag *et al.*, 2011a and 2011b), were also investigated.

This study describes the organically complexed state of Fe over the whole water column and the observed changes in the Fe chemistry when passing from the Sub-Antarctic Ocean into the Weddell Gyre (HNLC regions). With the knowledge of the Fe chemistry and of the organically complexed Fe in the whole water column, the processes controlling the Fe distribution in the world oceans can be better understood.

2. Description of the Southern Ocean

2.1. General aspects of the Southern Ocean

Many special aspects of the Southern Ocean give it a unique status. First of all, it is the only ocean with a permanent water flow around the globe (Antarctic Circumpolar Current, ACC), and the only ocean that communicates directly with the Atlantic Ocean, the Pacific Ocean and the Indian Ocean. The Southern Ocean is a key place for the deep water formation and thus for thermohaline circulation (Carmack, 1977; Mantyla and Reid, 1983; Foldvik and Gammelrød, 1988; Orsi *et al.*, 1999).

2.2. Fronts and zones

Several fronts (Figure 1) separate the Southern Ocean in different zones (Pollard *et al.*, 2002). The bottom topography contributes in maintaining the division of these zones with ridges separating different basins. Along the Zero Meridian, the Sub-Tropical Front (STF) with a surface salinity of 34.8 (Whitworth and Nowlin, 1987) and a temperature of 10-12ºC at 200 m depth separates warmer South Atlantic Surface Water (SASW) from the cooler and fresher Sub-Antarctic Surface Water (SAASW) in the Sub-Antarctic Zone (SAZ). Southwards, the Sub-Antarctic Front (SAF) separates the SAZ from the Polar Frontal Zone (PFZ) with a drop in salinity (Whitworth and Nowlin, 1987). During the ANTXXIV/3 cruise the SAF was located north of station 103 at ~46ºS (Figure 1). The PF is defined by a temperature of 2ºC at 200 m (Pollard *et al.*, 2002) and was located at 50º16'S just north of station 107. The Antarctic Zone (AAZ) is located on the Bouvet Triple Junction region (Atlantic-Indian Ridge which

separates the South Atlantic Basin and the Weddell Basin) and is delimited northwards by the Polar Front (PF) and southwards by the Southern Boundary (SB). The SB was located between 55º30'S and 56ºS on the Zero Meridian. The eastwards flowing ACC is found between the SAF and the SB. The Weddell Gyre is located between the SB and the Antarctic continent (Pollard *et al.*, 2002).

2.3. Water masses

2.3.1. Along the Zero Meridian

At the surface, the South Atlantic Surface Water (SASW, warm >12ºC, Whitworth and Nowlin, 1987) is found north of the STF and the Sub-Antarctic Surface Water (SSW) is found in the SAZ. The North Atlantic Deep Water (NADW, colder and more saline) flows along the bottom in the SAZ and PFZ. The Antarctic Intermediate Water (AAIW) flows northwards between the NADW and the surface water north of the PF. In the AAZ, the Circumpolar Deep Water is the main water mass present and is divided into the Upper Circumpolar Deep Water (UCDW) and the Lower Circumpolar Deep Water (LCDW). South of the SB (55ºS), in the Weddell Gyre the Antarctic Surface Water (AASW) coming from the ice melting during the summer (<5ºC) and the Antarctic deep water (colder and more saline) are found. This last water mass is divided into 3 separated water masses (Carmack and Foster, 1975; Fahrbach *et al.*, 2004; Klatt *et al.*, 2005), the Warm Deep Water (WDW) between ~200-1000 m with positive temperatures, the Weddell Sea Deep Water (WSDW, temperatures between 0ºC and -0.7ºC) and the Weddell Sea Bottom Water (WSBW, temperature below -0.7ºC).

2.3.2. In the Weddell Gyre

The Weddell Sea is an important region in the Southern Ocean because it is the main location where the Antarctic bottom water is formed (Klatt *et al.*, 2005). The cold surface water sinks along the continental slope of the Antarctic Peninsula towards the bottom and circulates eastwards along the North Weddell Ridge and the Southern Indian Ridge. The Weddell Gyre is limited westwards by the Antarctic Peninsula (60ºW) and extends eastwards along the North Weddell Ridge (60ºS) and along the

Southwest Indian Ridge (50-55ºS) until the Enderby Basin at 30ºE (Deacon, 1979; Gouretski and Danilov, 1993). The circulation of the water in the Weddell Gyre is cyclonic. The Weddell Sea is mainly constituted of the WDW, WSDW and WSBW. On top is the surface water (SW) about 100-200 m thick, with negative temperatures due to sea-ice melting.

2.3.3. Through the Drake Passage

The Drake Passage is a relatively narrow pathway between South America and the Antarctic Peninsula where the Antarctic Circumpolar Current and the South Pacific Currents converge. In this passage, the ACC is the main water mass present and is divided into the UCDW and the LCDW. The South Pacific Deep Water (SPDW), dense and characterised by high concentration of SiO_4, is also found (Sievers *et al.*, 1984). The Weddell Sea Bottom Water is also found in the Drake Passage. After bypassing the Antarctic Peninsula, the WSBW follows the bottom topography and circulates westwards along the continental slope in the Drake Passage.

3. Additional details on the materials and methods

3.1. Cruise track and sampling strategy

The ANT XXIV/3 expedition onboard R.V. *Polarstern* started from Cape Town, South Africa (February 2008), going south-westwards and reached the Zero Meridian at ~50ºS (Figure 1). The Sub-Tropical Front (STF), the Sub-Antarctic Front (SAF), the Polar Front (PF) and the Southern boundary of the Antarctic Circumpolar Current (SB in the present study) were successively crossed on the Zero Meridian. The Southern Boundary is also called SBdy in the Drake Passage by others (Barré *et al.*, 2008). The expedition continued across the Weddell Sea to King Georges Island, and finally traversed the Drake Passage until arrival in Punta Arenas, Chile (April 2008).

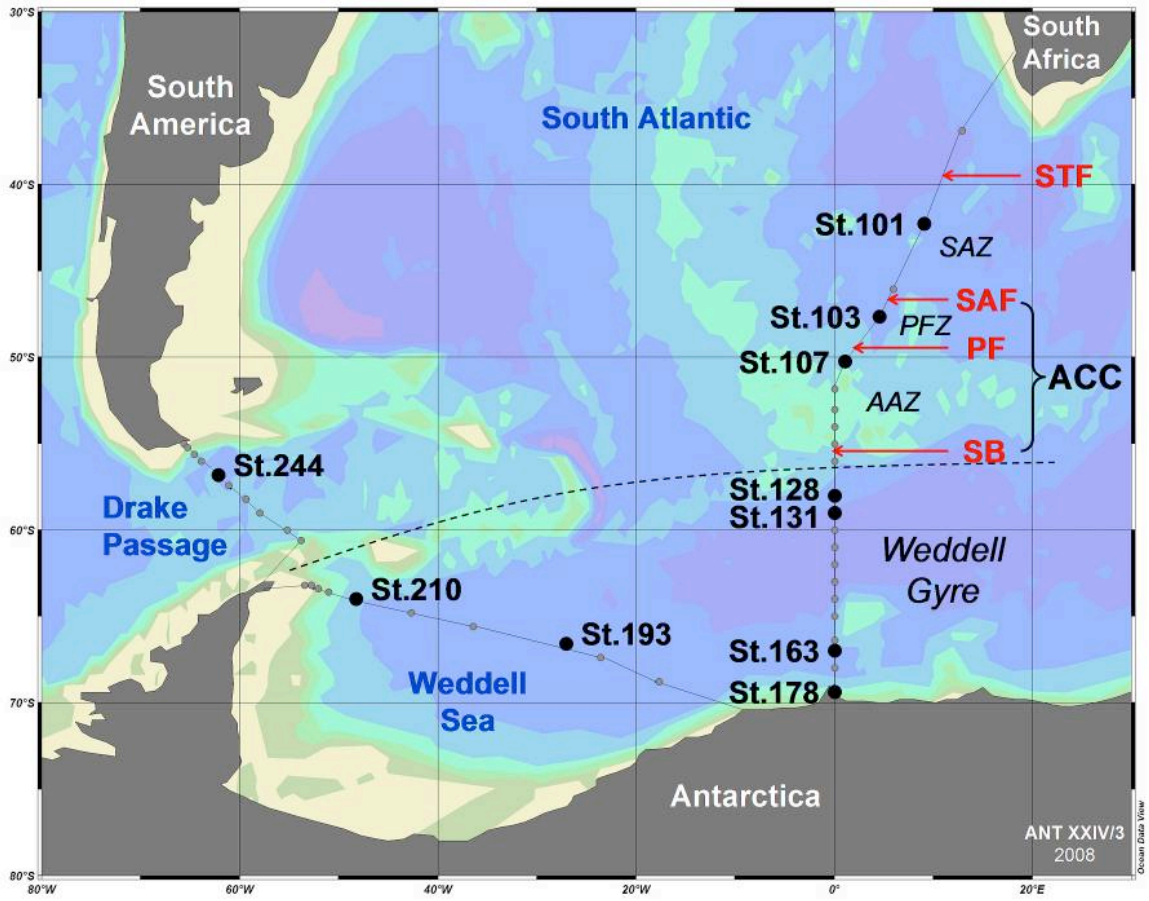

Figure 1: *Chart of the Atlantic sector of the Southern Ocean and location of the fronts and zones. The 10 stations sampled for this study are indicated by large black dots with station numbers. The small grey dots represent the additional stations also sampled with the titanium frame from NIOZ. The dashed line delimits the Weddell Gyre. STF = Sub-Tropical Front; SAF = Sub-Antarctic Front; PF = Polar Front; SB = Southern Boundary; SAZ = Sub-Antarctic Zone (St. 101); PFZ = Polar Frontal Zone (St. 103); AAZ = Antarctic Zone (St. 107); ACC = Antarctic Circumpolar Current; Weddell Gyre (St. 128, 131, 163, 178, 193 and 210.*

Overall 10 stations were sampled (Figure 1), for a total of 82 samples: 7 stations along the Zero Meridian, 2 stations in the Weddell Sea and 1 station in the Drake Passage. Station 101 was located in the SAZ (42.34ºS), station 103 in the PFZ (46ºS), station 107 in the AAZ south of the PF (50.27ºS). Stations 128 (58ºS), 131 (59ºS), 163 (67ºS) and 178 (69.4ºS) were situated in the eastern part of Weddell Gyre on the Zero Meridian. The stations 193 and 210 were taken in the Weddle Sea. The station 244 was located north of the PF in the Drake Passage (between 57º41'S and 57º51'S) and south of the SAF. Each sample was taken at judiciously chosen depths in order to sample all the different water masses present.

3.2. Fluorescence

Fluorescence, given in arbitrary unit (a.u.), was obtained from the NIOZ CTD sensor installed on the titanium frame. It corresponds to chlorophyll-a and is an indicator of phytoplankton abundance in seawater (Kiefer *et al.*, 1973; Babin *et al.*, 1996). Note that we discuss the layer where the fluorescence is >0.1 a.u. as the euphotic layer (this chapter and next chapters). The euphotic layer is defined as the depth range where the measured Photosynthetic Active Radiation (PAR) is more than 1 % of the incoming PAR at the sea surface (*i.e.* from sea surface until the 1% light depth) and is slightly different to the depth where the fluorescence was >0.1 a.u.. We did so to combine the influence of the light irradiance and of the presence of phytoplankton.

Table 1: *Averaged fluorescence (arbitrary unit, a.u.) in the surface layer per station. Standard deviations (S.D.), the number of samples (n) and the maximum depth (m) where* fluorescence > 0.1 a.u. are shown.

Stations	Fluorescence (a.u.)	S.D.	n	Maximum depth (m)
101	0.41	0.21	6	100
103	0.59	0.26	5	75
107	0.30	0.02	6	100
128	0.27	0.04	5	90
131	0.11	0.01	4	100
163	0.94	0.51	6	100
178	1.01	0.97	7	140
193	0.42	0.17	6	100
210	0.16	0.01	4	50
244	0.24	0.02	7	100

Relatively high values in surface waters corresponding to a chlorophyll maximum at about 50 m depth (euphotic zone) and a decrease with depth towards the aphotic zone were observed. At station 178 the fluorescence could even be detected at ~140 m depth.

Table 1 shows the average of fluorescence in the surface layer per station when it was > 0.1 a.u.. Stations 101 and 103 had relatively high fluorescence compared to stations 131 and 210 where lower fluorescence was recorded. Close to the ice edge

(St. 163 and 178) the highest fluorescence of all stations was measured due to a phytoplankton bloom.

4. Results

4.1. Dissolved Fe distribution

The concentrations of dissolved Fe along the Zero Meridian (Figure 2 and Table 2) from the same expedition are shown in detail by Klunder *et al.* (2011). At the stations presented here, the concentration of dissolved Fe was always below the nano-molar level and showed a nutrient-like vertical profile.

With a surface minimum at all stations (between 0.02 and 0.19 nM) the concentration of dissolved Fe increased with depth with a maximum just above the seafloor (St. 163: 0.58 nM; St. 193: 0.59 nM), or became more or less constant below 500-1000 m (St. 101: 0.63 nM; St. 103: 0.56 nM; St. 131: 0.36 nM; St. 244: 0.40 nM). Station 107 located south of the PF showed variability in the concentrations of dissolved Fe in the upper layers (0-450 m). It remained constant below 450 m at ~0.55 nM. At station 128 a steep increase was found from the surface until 450 m (until 0.76 nM) followed by a minimum at 1000 m (0.35 nM), and by a second maximum at 2500 m (0.68 nM) and a decrease towards the bottom. Two samples were taken at station 178 in the upper water at 137 and 451 m depth with 0.08 and 0.17 nM of Fe, respectively. Station 210 close to the Antarctic Peninsula slope had a maximum concentration of Fe between 1000 and 1500 m (0.46 nM) ascribed to hydrothermal input (Klunder *et al.*, 2011).

Table 2 (Below and next page): *Dissolved Fe and the characteristics of the dissolved Fe binding ligands of all samples. Dissolved Fe concentrations [DFe] are in nM (± standard deviations). Concentrations of the ligand [Lt] and the excess ligand [L'] are in Eq of nM Fe (± standard deviations). Conditional stability constants K' are in mol^{-1} with standard deviations.*
At station 101 the deepest samples collected at 3505 m and 4353 m had higher values of dissolved Fe, 0.630 nM and 0.572 nM, respectively, as compared with the duplicate sub-samples reported by Klunder et al. (2011), 0.401 nM and 0.280 nM, respectively.

The cause for this discrepancy is not known; perhaps our samples were contaminated. Nevertheless here we use our values, 0.63 nM and 0.572 nM in further interpretation. At station 178 Klunder et al. (2011) measured a complete vertical profile and found elevated concentrations of dissolved Fe between 300 and 800 m depth due to melted ice (1.50 nM of Fe at 451 m). The cause for the discrepancy with our sample at 451 m (0.171 nM) is not known.

** when the [DFe] was not determined in the same sample and therefore the concentration [DFe] was averaged from the samples above and under it; this was used for the calculation of the ligand characteristics (Eq. 2).*

***The standard deviation for Fe concentrations is missing when there was not enough sample volume to determine the concentration in triplicate.*

Station	Depth (m)	DFe (nM)	S.D.	[Lt] (Eq of nM Fe)	S.D.	log K' (mol^{-1})	S.D.	[L'] (Eq of nM Fe)	logα	pFe (M)	[Lt]/[DFe]
101											
	48	0.180	0.010	0.71	0.13	22.00	0.35	0.53	12.72	22.47	3.9
	76	0.105	0.007	0.53	0.10	22.12	0.24	0.43	12.76	22.73	5.1
	199	0.270	0.000	0.78	0.37	21.45	0.27	0.51	12.15	21.72	2.9
	502	0.377	0.004	0.70	0.18	21.69	0.33	0.32	12.19	21.62	1.9
	1001	0.587	0.017	1.17	0.11	21.66	0.09	0.59	12.43	21.66	2.0
	1502	0.540	0.020	1.25	0.13	22.16	0.21	0.71	13.02	22.28	2.3
	2501	0.630	0.030	1.26	0.11	21.91	0.13	0.63	12.71	21.91	2.0
	3505	0.630	0.000	1.07	0.05	22.61	0.20	0.44	13.26	22.46	1.7
	4353	0.572	0.039	0.92	0.09	22.42	0.29	0.35	12.97	22.21	1.6
103											
	45	0.187	0.005	0.70	0.20	22.39	0.41	0.51	13.10	22.82	3.7
	73	0.280	0.020	1.44	0.17	22.11	0.19	1.16	13.17	22.72	5.1
	203	0.318	0.015	1.12	0.14	22.40	0.25	0.81	13.30	22.80	3.5
	404	0.522	0.004	1.08	0.14	22.21	0.32	0.56	12.96	22.24	2.1
	499	0.536*	**	1.11	0.10	22.59	0.30	0.57	13.35	22.62	2.1
	751	0.551	0.025	0.90	0.16	22.18	0.35	0.35	12.72	21.98	1.6
	1253	0.532	0.008	0.90	0.08	22.38	0.26	0.37	12.94	22.22	1.7
	1747	0.540	**	1.13	0.10	22.74	0.28	0.59	13.51	22.78	2.1
	2001	0.582	0.009	1.55	0.18	21.93	0.18	0.96	12.92	22.15	2.7
	3099	0.560	0.006	0.99	0.08	22.34	0.22	0.43	12.98	22.23	1.8
107											
	49	0.096	0.002	0.87	0.19	21.84	0.36	0.77	12.73	22.75	9.1
	75	0.540	0.030	1.11	0.17	22.16	0.35	0.57	12.92	22.18	2.1
	199	0.199	0.008	0.84	0.16	21.69	0.16	0.64	12.50	22.20	4.2
	301	0.246	0.013	0.61	0.06	22.49	0.33	0.37	13.06	22.67	2.5
	499	0.520	0.020	0.97	0.07	22.31	0.17	0.45	12.96	22.25	1.9
	749	0.370	0.020	0.97	0.15	21.91	0.24	0.60	12.68	22.11	2.6
	1250	0.560	0.050	0.80	0.06	22.48	0.16	0.24	12.86	22.11	1.4
	1749	0.507	0.006	0.85	0.08	22.54	0.36	0.35	13.08	22.38	1.7
	3500	0.508	0.020	0.68	0.05	22.94	0.31	0.08	12.85	22.07	1.1

Station	Depth (m)	DFe (nM)	S.D.	[Lt] (Eq of nM Fe)	S.D.	log K' (mol^{-1})	S.D.	[L'] (Eq of nM Fe)	logα	pFe (M)	[Lt]/[DFe]
128											
	87	0.162	0.017	0.90	0.15	21.86	0.23	0.74	12.73	22.52	5.6
	311	0.490	0.010	1.84	0.33	21.74	0.23	1.35	12.87	22.18	3.8
	498	0.759	0.020	1.33	0.15	21.97	0.17	0.57	12.72	21.84	1.7
	1001	0.345	0.005	1.30	0.12	21.95	0.15	0.96	12.93	22.40	3.8
	1744	0.439	0.012	0.90	0.11	22.18	0.28	0.46	12.84	22.20	2.0
	2498	0.682	0.044	1.08	0.17	22.23	0.47	0.40	12.83	22.00	1.6
	3497	0.640	0.036	0.92	0.10	22.58	0.28	0.28	13.03	22.22	1.4
	4466	0.481	0.014	0.71	0.13	22.29	0.28	0.23	12.64	21.96	1.5
131											
	50	0.100	0.010	0.81	0.10	22.40	0.43	0.71	13.25	23.25	8.1
	152	0.133	0.003	0.98	0.19	21.68	0.21	0.84	12.60	22.48	7.3
	748	0.235	0.001	0.66	0.19	21.84	0.40	0.43	12.47	22.10	2.8
	1250	0.473	0.009	1.27	0.12	21.86	0.13	0.79	12.76	22.08	2.7
	1750	0.348	0.001	0.87	0.09	22.53	0.40	0.53	13.26	22.71	2.5
	3495	0.362	0.002	0.66	0.07	22.10	0.21	0.30	12.58	22.02	1.8
	4245	0.453	0.002	1.14	0.21	21.87	0.22	0.69	12.71	22.05	2.5
	4514	0.307	0.004	1.03	0.10	22.22	0.23	0.72	13.07	22.59	3.3
163											
	44	0.045	0.001	0.73	0.07	22.50	0.39	0.68	13.33	23.68	16.2
	101	0.107	0.006	0.67	0.13	22.16	0.54	0.56	12.91	22.88	6.3
	210	0.180	0.001	0.88	0.15	22.04	0.30	0.70	12.89	22.63	4.9
	300	0.192	0.001	0.75	0.10	22.32	0.35	0.56	13.07	22.78	3.9
	748	0.201	0.003	0.71	0.08	22.36	0.33	0.51	13.07	22.77	3.6
	1001	0.235	0.013	1.00	0.06	22.37	0.15	0.77	13.26	22.89	4.3
	1501	0.270	0.014	1.01	0.12	22.53	0.61	0.74	13.40	22.96	3.7
	2501	0.418	0.012	1.26	0.16	22.30	0.40	0.84	13.23	22.61	3.0
	4499	0.581	0.051	0.87	0.06	22.51	0.25	0.29	12.98	22.21	1.5
178											
	137	0.081	0.007	1.08	0.23	21.60	0.18	1.00	12.59	22.69	13.3
	451	0.171	0.005	0.88	0.14	21.93	0.24	0.71	12.79	22.55	5.2

Station	Depth (m)	DFe (nM)	S.D.	[Lt] (Eq of nM Fe)	S.D.	log K' (mol^{-1})	S.D.	[L'] (Eq of nM Fe)	logα	pFe (M)	[Lt]/[DFe]
193											
	50	0.045	0.001	1.33	0.17	22.20	0.35	1.28	13.31	23.66	26.7
	101	0.094	0.003	0.69	0.07	22.60	0.46	0.59	13.38	23.40	8.3
	402	0.192	0.009	1.31	0.13	22.24	0.25	1.11	13.29	23.00	6.7
	1000	0.211	0.006	1.25	0.11	22.18	0.19	1.04	13.20	22.87	5.8
	2001	0.327	0.002	1.32	0.19	22.12	0.26	0.99	13.12	22.60	4.0
	2998	0.390	0.021	1.10	0.09	22.76	0.55	0.71	13.61	23.02	2.8
	3997	0.534	0.003	1.39	0.09	22.43	0.21	0.86	13.36	22.63	2.6
	4799	0.592	0.015	1.52	0.09	22.34	0.16	0.93	13.31	22.53	2.6
210											
	30	0.030	0.010	0.49	0.06	22.56	0.43	0.46	13.22	23.73	15.8
	99	0.060	0.010	0.80	0.13	22.16	0.46	0.75	13.04	23.28	13.9
	249	0.160	0.000	1.24	0.09	22.34	0.20	1.08	13.37	23.16	7.7
	351	0.150	0.010	0.92	0.06	22.23	0.16	0.77	13.12	22.94	6.2
	750	0.240	0.010	1.03	0.15	22.17	0.21	0.79	13.07	22.70	4.3
	1000	0.460	0.020	1.16	0.06	22.64	0.23	0.69	13.48	22.81	2.5
	1501	0.460	0.020	1.20	0.07	22.44	0.12	0.75	13.31	22.66	2.6
	2000	0.310	0.020	1.54	0.07	22.24	0.10	1.23	13.33	22.84	5.0
	3500	0.320	0.010	1.08	0.10	22.12	0.19	0.76	13.00	22.50	3.4
	3946	0.360	0.010	1.13	0.05	22.34	0.11	0.77	13.22	22.67	3.2
244											
	38	0.021	0.001	1.38	0.11	21.90	0.12	1.36	13.03	23.71	66.9
	73	0.172	0.005	1.38	0.06	22.78	0.30	1.21	13.87	23.63	8.0
	147	0.128	0.011	1.38	0.11	22.30	0.22	1.25	13.40	23.29	10.8
	748	0.276	0.005	1.45	0.10	22.14	0.15	1.17	13.21	22.76	5.2
	1250	0.381	0.007	1.32	0.13	22.50	0.36	0.94	13.47	22.89	3.5
	1749	0.405	0.024	1.36	0.08	22.11	0.12	0.96	13.09	22.48	3.4
	2497	0.361	0.019	1.34	0.10	22.16	0.16	0.98	13.15	22.59	3.7
	3501	0.441	0.021	1.37	0.08	22.18	0.12	0.93	13.15	22.51	3.1
	4002	0.362	0.002	1.00	0.08	22.59	0.33	0.64	13.40	22.84	2.8

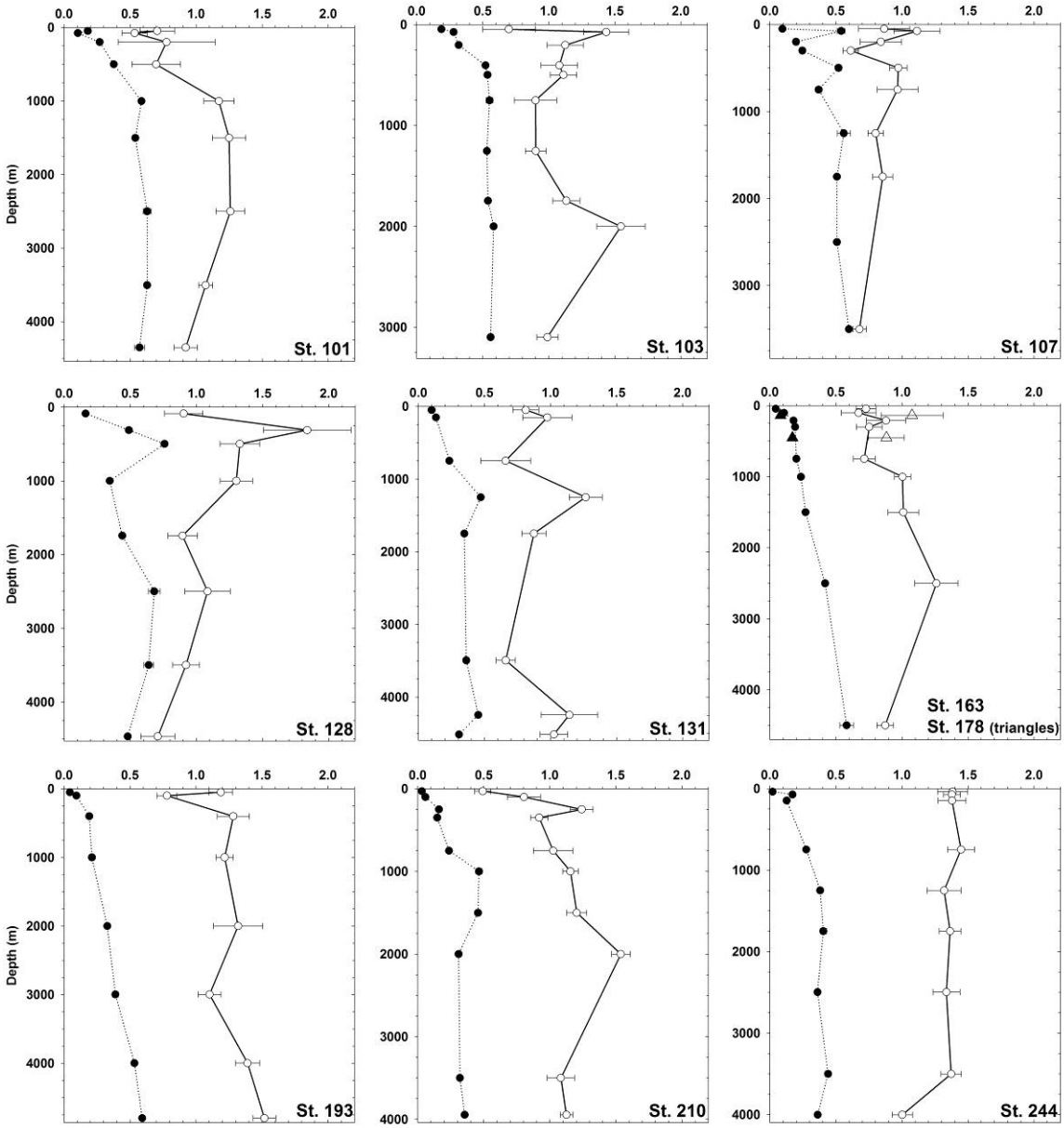

Figure 2: *Vertical distribution of organic ligands (white dots, solid line) and of dissolved Fe (black dots, dotted line) for the 10 stations. Station 163 and 178 (triangles at 137 and 451 m) are plotted in the same graph. Ligand concentrations are in Eq of nM Fe and dissolved Fe concentrations are in nM. The vertical axes are extended until the bottom depth.*

4.2. Organic ligand distribution and characteristics

The concentration of ligands (Figure 2 and Tables 2 and 3) throughout the water column ranged between 0.49 and 1.84 Eq of nM Fe (nano Equivalents of molar Fe). The upper 450 m showed relatively variable ligand concentrations. At stations 101, 131, 163 and 193 the concentrations were between 0.5 and 1.2 Eq of nM Fe in the first

450 meters. At stations 103, 107, 128 and 210 a maximum (1.1-1.9 Eq of nM Fe) was observed between 70 and 310 m depth after a surface minimum (0.5-0.9 Eq of nM Fe). Below 450 m depth the concentration of ligand decreased towards the bottom at station 101, 107 and 128. The ligand concentration was relatively constant at station 163. Station 131 showed higher concentrations of ligand near the seafloor (around 1.09 Eq of nM Fe). The concentration of ligand increased gradually towards the seafloor in the Weddell Sea at stations 193 and 210. At station 244, the concentration of ligand was stable from the surface until 3500 m around 1.33 Eq of nM Fe. Near the seafloor it was about 1.00 Eq of nM Fe.

The concentration of excess ligand (Excess L = L') with respect to Fe ([Lt]-[DFe], Table 2) corresponds to the concentration of free Fe binding sites. A small value of excess L means a near saturation of the ligand. In the upper layer (0-450 m) the mean values of excess L were 0.62 Eq of nM Fe north of the SB, 0.79 Eq of nM Fe in the Weddell Gyre on the Zero Meridian, 0.85 Eq of nM Fe in the Weddell Sea and 1.27 Eq of nM Fe in the Drake Passage (Table 3). Below 450 m depth, the averaged concentrations of excess L were 0.47, 0.56, 0.86 and 0.94, respectively, for the same zones. A surface maximum in excess L was usually found (St. 101, 107, 131, 163, 193 and 244). This excess L increased on average southwards the Southern Boundary on the Zero Meridian. More excess L was found close to the Antarctic ice-edge as well as in the Weddell Sea and in the Drake Passage.

The binding strength is defined by the conditional stability constant K' (Table 2). The K' ranged between $10^{21.45}$ and $10^{22.94}$. The value of K' was variable in the first 500-1000 m in all stations and it slightly increased with depth on the Zero Meridian. At station 193 in the Weddell Sea, K' was also variable with high values of K' at 750 m depth ($10^{22.82}$) and at 3000 m depth ($10^{22.76}$). At station 210, K' was constant over the water column, except at the surface and at 1000 m where higher values were found. In the Drake Passage, the value of K' was constant ($10^{22.15}$) over the water column except for the shallowest and deepest samples.

The organic alpha was relatively constant (about 10^{13}) from 450 m depth towards the bottom at all stations. Variable values of organic alpha were found in the first 450 m layer, ranging from 10^{12} at station 101 to $10^{13.5}$ at station 244. Below 450 m depth at

the stations north of the SB and in the north part of the Weddell Gyre (until station 131) the values of organic alpha were smaller than 10^{13}. Below 450 m depth at the stations close to the Antarctic ice edge, in the Weddell Sea and in the Drake Passage the values of organic alpha were larger than 10^{13} due to higher excess L in these regions.

Relatively low pFe values (Table 2) corresponding to relatively high Fe^{3+} concentrations are due to lower organic alpha values and thus either weaker ligands or lower concentrations of excess L. At stations 101 until 131, pFe decreased from 22.5-23 at the surface to approximately 22 at 450 m depth and remained constant towards the bottom. At stations 163, 193, 210 and 244, a decrease in pFe from 23.7-23.8 at the surface to 22.2-22.5 near the seafloor was found.

The ratio [Lt]/[DFe] (Figures 3 and 4, Tables 2 and 3) shows how much more ligand there is compared to the dissolved Fe. If [Lt]/[DFe] = 1, the ligand sites are fully saturated with Fe. The ratio [Lt]/[DFe] is a useful concept to highlight differences in ligand saturation throughout the water column and between different geographical locations (Thuroczy *et al.*, 2010b and Chapter 3). In order to discuss separately the phenomena and processes occurring in the ocean, the boundary between the upper and deeper ocean was operationally defined at 450 m depth. This choice was dictated by the sampling depths, as the samples were usually taken at fixed depth (…400, 500, 750 m depth…).

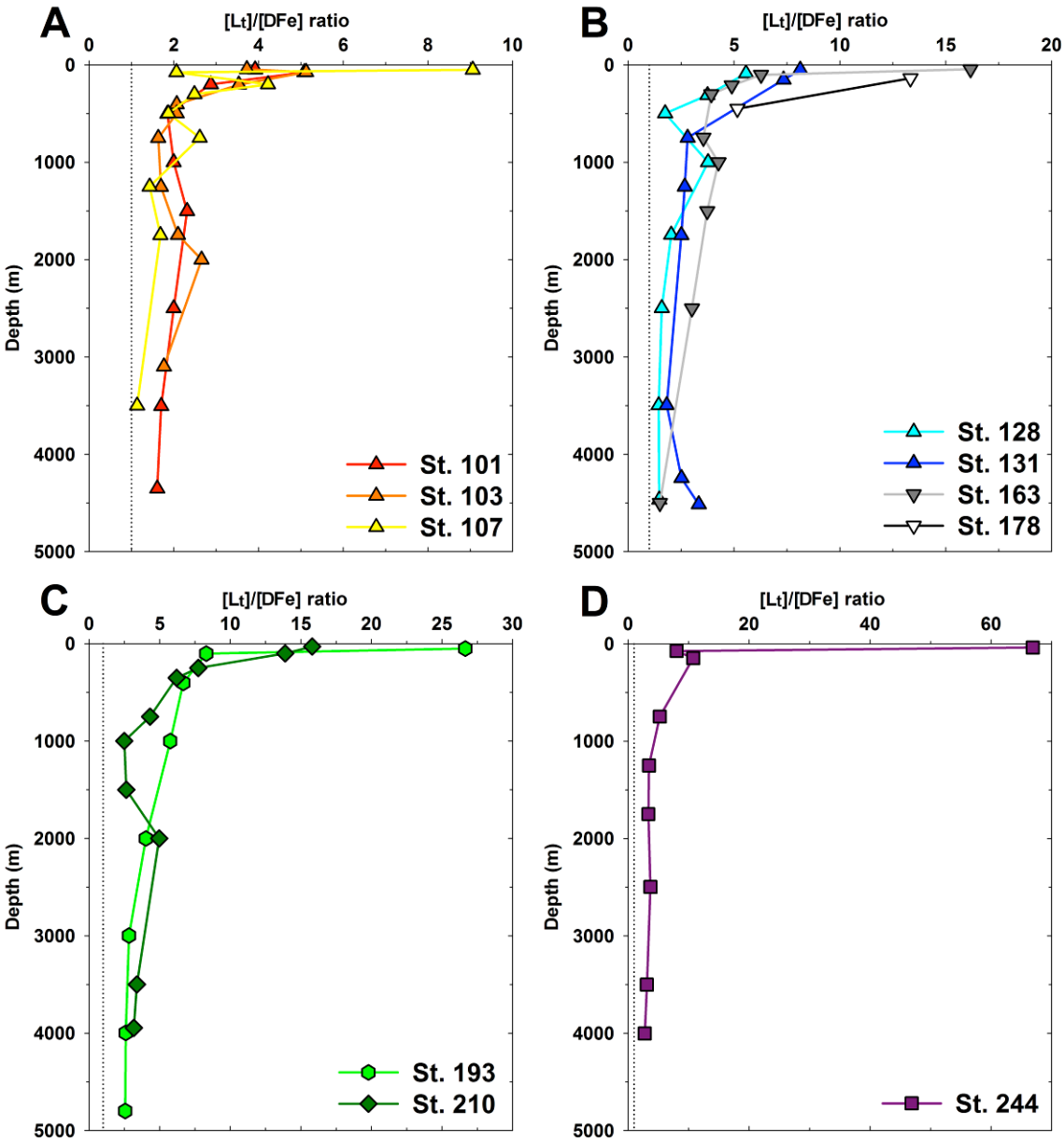

Figure 3: *Ratio values of [Lt]/[DFe]. **A:** North of the SB; **B:** Weddell Gyre on the Zero Meridian; **C:** Weddell Sea; **D:** Drake Passage. The dotted line marks exact saturation of the ligand with [Lt]/[DFe] = 1. Note the different scales on the horizontal axis for the ratio values.*

Table 3: *Average and standard deviation of [Lt] (Eq of nM Fe), [DFe] (nM), [L'] (Eq of nM Fe) and the ratio [Lt]/[DFe] per station and per zone.* ***A:*** *in the upper layer (0-450 m).* ***B:*** *in the deeper part of the ocean (below 450 m depth).* ***C:*** *subdivision of the upper layer for [Lt]/[DFe]: samples from the surface are shown separately from those in the euphotic layer (where fluorescence > 0.1 a.u., surface sample included) and in the layer below it until 450 m depth (Intermediate layer).*
** indicates large standard deviation (Station 244) due to the extremely high surface ratio [Lt]/[DFe] (66.9) compared to the value below this.*

A			Upper layer (0 - 450 m)							
Zones		Stations	Number of samples	Average [Lt]	S.D.	Average [DFe]	S.D.	Average [L']	S.D.	Average [Lt]/[DFe]	S.D.
↑	North of SB	101	n = 3	0.67	0.12	0.185	0.083	0.49	0.05	4.0	1.1
		103	n = 4	1.08	0.30	0.327	0.141	0.76	0.29	3.6	1.2
		107	n = 4	0.86	0.21	0.270	0.191	0.59	0.17	4.5	3.2
Prime Meridian		Average	n = 11	**0.89**	**0.27**	**0.267**	**0.147**	**0.62**	**0.22**	**4.0**	**2.0**
	↑	128	n = 2	1.37	0.66	0.326	0.232	1.04	0.43	4.7	1.3
		131	n = 2	0.89	0.12	0.116	0.023	0.78	0.09	7.7	0.6
		163	n = 4	0.76	0.09	0.131	0.068	0.63	0.07	7.8	5.7
↓	Weddell Gyre	178	n = 2	0.98	0.14	0.126	0.064	0.85	0.20	9.2	5.8
		Average	n = 10	**0.95**	**0.33**	**0.166**	**0.123**	**0.79**	**0.23**	**7.5**	**4.1**
Weddell Sea		193	n = 3	1.08	0.27	0.110	0.075	0.97	0.25	13.9	11.1
		210	n = 4	0.86	0.31	0.099	0.064	0.77	0.25	10.9	4.7
	↓	Average	n = 7	**0.96**	**0.29**	**0.104**	**0.063**	**0.85**	**0.26**	**12.2**	**7.4**
Drake Passage		244	n = 3	1.29	0.18	0.131	0.079	1.27	0.08	28.6	33.2*

B			Deeper layer (below 450 m)							
Zones		Stations	Number of samples	Average [Lt]	S.D.	Average [DFe]	S.D.	Average [L']	S.D.	Average [Lt]/[DFe]	S.D.
↑	North of SB	101	n = 6	1.06	0.22	0.556	0.094	0.51	0.16	1.9	0.3
		103	n = 6	1.10	0.24	0.550	0.019	0.55	0.23	2.0	0.4
		107	n = 5	0.85	0.12	0.511	0.077	0.34	0.20	1.7	0.6
Prime Meridian		Average	n = 17	**1.01**	**0.22**	**0.539**	**0.070**	**0.47**	**0.20**	**1.9**	**0.4**
	↑	128	n = 6	1.04	0.24	0.558	0.160	0.48	0.26	2.0	0.9
		131	n = 6	0.94	0.25	0.363	0.089	0.58	0.19	2.6	0.5
		163	n = 5	0.97	0.20	0.341	0.158	0.63	0.23	3.2	1.1
↓	Weddell Gyre	Average	n = 17	**0.98**	**0.22**	**0.425**	**0.164**	**0.56**	**0.22**	**2.6**	**0.9**
Weddell Sea		193	n = 5	1.25	0.20	0.376	0.162	0.90	0.12	3.6	1.4
		210	n = 6	1.19	0.18	0.357	0.089	0.83	0.20	3.5	1.0
	↓	Average	n = 11	**1.24**	**0.17**	**0.382**	**0.119**	**0.86**	**0.16**	**3.5**	**1.1**
Drake Passage		244	n = 6	1.31	0.16	0.371	0.055	0.94	0.17	3.6	0.9

C			Subdivision of the upper 450 m in:								
			Surface sample			Euphotic layer (where fluorescence > 0.1 a.u.)			Intermediate layer (where fluorescence < 0.1 a.u.)		
Zones		Stations	Depth (m)	Number of samples	[Lt]/[DFe]	Depth (m)	Number of samples	Average [Lt]/[DFe]	Depth (m)	Number of samples	Average [Lt]/[DFe]
↑	North of SB	101	48	n = 1	3.9	0 - 100	n = 2	4.5 ± 0.8	100 - 450	n = 1	2.9
		103	45	n = 1	3.7	0 - 75	n = 2	4.4 ± 1.0	75 - 450	n = 2	2.8 ± 1.0
		107	49	n = 1	9.1	0 - 100	n = 2	5.6 ± 4.9	100 - 450	n = 2	3.4 ± 1.2
Prime Meridian		Average		n = 3	**5.6 ± 3.0**		n = 6	**4.8 ± 2.4**		n = 5	**3.0 ± 0.9**
	↑	128	87	n = 1	5.6	0 - 90	n = 1	5.6	90 - 450	n = 1	3.8
		131	50	n = 1	8.1	0 - 100	n = 1	8.1	100 - 450	n = 1	7.3
		163	44	n = 1	16.2	0 - 100	n = 2	11.2 ± 7.0	100 - 450	n = 2	4.4 ± 0.7
↓	Weddell Gyre	178				0 - 140	n = 1	13.3	140 - 450	n = 1	5.2
		Average		n = 3	**10.0 ± 5.5**		n = 5	**9.9 ± 4.6**		n = 5	**5.0 ± 1.4**
Weddell Sea		193	50	n = 1	26.7	0 - 100	n = 2	17.5 ± 13	100 - 450	n = 1	6.7
		210	30	n = 1	15.8	0 - 50	n = 1	15.8	50 - 450	n = 3	9.3 ± 4.2
	↓	Average		n = 2	**21.2 ± 7.7**		n = 3	**16.9 ± 9.2**		n = 4	**8.6 ± 3.6**
Drake Passage		244	38	n = 1	66.9	0 - 100	n = 2	37.5 ± 41.6*	100 - 450	n = 1	10.8

A trend was seen in the [Lt]/[DFe] ratio with depth in the water column. High [Lt]/[DFe] ratio values were found at the surface with a decrease until 450 m (Figures 3 and 4, Table 3). The upper layer (0-450 m) was characterised by low dissolved Fe

concentrations (surface minima) and variable ligand concentrations. To highlight the steep decrease of the ratio [Lt]/[DFe] from the upper layer downwards, the ratios of the samples from the surface, *i.e.* the samples where phytoplankton grew (fluorescence > 0.1 a.u., Table 1) and of the layer underneath until 450 m depth (fluorescence < 0.1 a.u.) are shown separately in Table 3C.

Below 450 m depth the ratios [Lt]/[DFe] were lower and more constant with depth. This deeper part appeared to be a relatively stable environment (constant concentrations of dissolved Fe and of ligand) where degradation and remineralisation of the organic matter were the dominant chemical processes. A trend in [Lt]/[DFe] between geographical locations was also seen (Figures 3 and 4, Table 3). The ratio values [Lt]/[DFe] increased on average over the whole water column southwards the Southern Boundary on the Zero Meridian and from east to west in the Weddell Gyre.

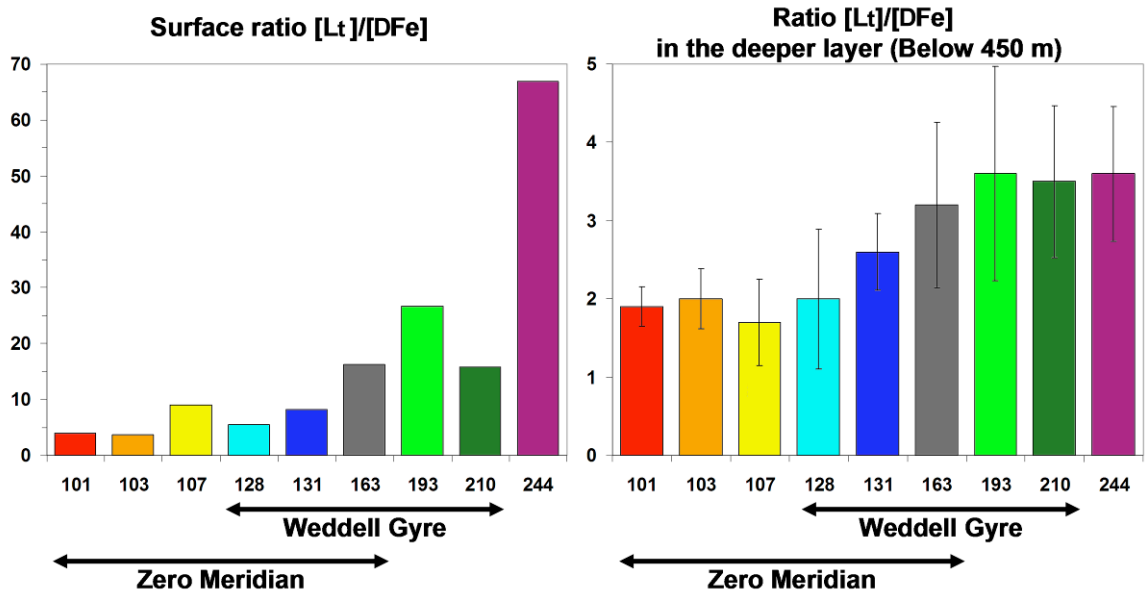

Figure 4: *Values of [Lt]/[DFe] per station. On the left side: surface values of [Lt]/[DFe]. On the right side: averaged values of [Lt]/[DFe] with standard deviations in the layer below 450 m depth. Station 178 is not shown here since only 2 samples were taken (137 m and 451 m depth).*

5. Discussion

5.1. Comparison with literature

The ligand concentrations presented here are similar to the 0.4 and 1.4 Eq of nM Fe reported for the upper 1000 m at 2 stations close to the ice edge at 0º and 10ºW by Boye *et al.* (2001) and along the 20ºE in the ACC. Surface water (until 100 m depth) ligand and Fe concentrations published by Boye *et al.* (2005) from the EisenEx experiment were also comparable at 0.5-0.7 Eq of nM Fe and 0.05 nM, respectively. In addition, similar Fe speciation was estimated (between 0.5 and 1.5 Eq of nM Fe) for the Kerguelen Archipelago Plateau in the Southern Ocean by Gerringa *et al.* (2008), with the exception of the deepest samples. These higher ligand concentrations at depth were attributed to the influence of the sediments. Only at station 131 were the ligand concentrations found below 4000 m similar to those measured by Gerringa *et al.* (2008).

The K' values for the entire water column calculated by Gerringa *et al.* (2008) using the same method were lower ($< 10^{22}$) than the K' values estimated here (mainly $> 10^{22}$). At 55º49'S-6º1'E Croot *et al.* (2004b) found, below a surface minimum (1 Eq of nM Fe), a decrease in the concentration of ligand from 2.5 Eq of nM Fe at 30 m depth to 1.2 Eq of nM Fe at 400 m. This result is comparable to station 128 located in the same area. The K' values found by Croot *et al.* (2004b) were also similar (around 10^{22}) to those found here in the upper 400 m. The dissolved organic ligand characteristics observed during the present study and by others (Powell and Donat, 2001; Gerringa *et al.*, 2008) did not indicate differences between water masses.

5.2. Upper layer of the ocean (0-450 m)

The trend of an increasing [Lt]/[DFe] ratio in the upper waters (Tables 3A and 3C, Figure 4) from north to south on the Zero Meridian and from east to west in the Weddell Gyre probably reflects the existing phytoplankton regimes (Sub-Antarctic region and HNLC region). The high surface ratio confirms the importance of phytoplankton in increasing the ratio [Lt]/[DFe], by Fe uptake and probably ligand production. Both the concentrations of dissolved Fe and of ligands explain the difference in ratios [Lt]/[DFe], lower north of the SB and higher in the Weddell Gyre.

Within the Weddell Gyre, the increase in [Lt]/[DFe] ratio from east to west was due to a decrease in the concentration of dissolved Fe only. Lower concentrations of dissolved Fe were found in the Weddell Sea proper (0.10 nM, n = 7) as compared to those found in the Weddell Gyre on the Zero Meridian (0.17 nM, n = 10). The concentrations of ligand and excess L were relatively constant in the Weddell Gyre. The values of organic alpha and pFe also showed a trend in the upper layer between geographical locations. The increase of organic alpha from north to south on the Zero Meridian and from east to west in the Weddell Gyre was due to an increase in excess L, whereas the increase in pFe value in the upper layer was due to a decrease of the dissolved Fe concentration and an increase of the organic alpha. Station 244, located in the Drake Passage, showed the highest [Lt]/[DFe] ratio at the surface caused by both a high ligand concentration relative to a very low dissolved Fe concentration (0.021 nM). The trend of the ratio [Lt]/[DFe] between geographical locations is seen in the ratio [Lt]/[DFe] of the surface samples (0-50 m) (Table 3C), but also in the euphotic layer (fluorescence > 0.1 a.u.) and in the layer below this (fluorescence < 0.1 a.u.).

The high [Lt]/[DFe] at the surface can be explained by the uptake of Fe and production of ligands (relatively high and variable ligand concentrations) by phytoplankton in the euphotic layer and by the microbial activity degrading the non-resistant ligands (Rue and Bruland, 1997; Tortell *et al.*, 1999; Boye and Van Den Berg, 2000; Croot *et al.*, 2001; Gerringa *et al.*, 2006). The ligand concentration represents the difference between the production and the degradation of the Fe-binding molecules (Boye *et al.*, 2001).

The stations were located in regions influenced by different “regimes” in terms of primary production. The regime in the surface waters at stations 101, 103 and 107 (Sub-Antarctic region) is thus very different from the other stations. Relatively low [Lt]/[DFe] ratio values were found at these stations. Relatively high fluorescence was measured here and Fe was not a limiting factor for phytoplankton growth at these 3 stations. Moreover, the dissolved organic ligand concentration was lower here. This indicated that there was no (need for) production of ligands like siderophores by prokaryotes.

The stations located in the HNLC regions (128, 131, 163, 178, 193 and 210) had low dissolved Fe concentrations and relatively constant ligand concentrations, resulting in higher [Lt]/[DFe] ratio values. Near the edge of the Antarctic ice sheet even higher [Lt]/[DFe] ratio values were found. Here a phytoplankton bloom was clearly observed by high fluorescence at station 163 and 178 (Table 1): a source of Fe was apparently available since the bloom had started. The melting of the Antarctic ice-sheet, its calving icebergs and of the seasonal sea-ice was shown to be a source of dissolved Fe in seawater by Klunder *et al.* (2011). This extra Fe was consumed resulting in low dissolved Fe concentrations. Here, the ligand concentration was relatively constant and was not responsible for the high [Lt]/[DFe] ratio values. However, in the Weddell Sea, even higher ratios [Lt]/[DFe] were found at the surface, whereas, the fluorescence in the water was low. Low dissolved Fe concentrations occurring here explained this high ratio [Lt]/[DFe]. The low dissolved Fe concentration might be caused by a phytoplankton bloom in the recent past or more probably Fe is taken up by phytoplankton living in the sea-ice. The Weddell Sea is known to be a productive area with high biological diversity supported by the growth of phytoplankton in the sea-ice (Arrigo *et al.*, 1997; Flores, 2009). So, even if relatively low fluorescence was measured in the water, Fe consumption should be high.

The particulate fraction, an important part of the Fe cycle, is still missing in the present study and should help to explain the processes occurring in the upper ocean. Adsorption sites on suspended particles compete with empty ligand sites in the dissolved fraction for Fe (Thuróczy *et al*, 2010b and Chapter 3). The adsorption on suspended particles followed by aggregation and downward settling of these particles is deemed to be responsible for the removal of Fe by scavenging.

5.3. Deeper part of the ocean (below 450 m)

Below 450 m depth, the values of [Lt]/[DFe] were low and constant with depth. Like the upper layer (0-450 m depth), the deeper part of the water column also showed a geographical trend: an increase of the ratio [Lt]/[DFe] southwards the Southern Boundary on the Zero Meridian and from east to west in the Weddell Gyre.

The difference between Zero Meridian and Weddell Sea was due to a lower concentration of ligand (1.00 of Eq of nM Fe, n = 34; versus 1.24 Eq of nM Fe, n = 11, respectively). The southward decrease in dissolved Fe concentration on the Zero Meridian was due to an absence of Fe sources (Klunder *et al.*, 2011). Moreover, excess L increased southwards along the Zero Meridian, thus reinforcing the same trend in [Lt]/[DFe]. Within the Weddell Gyre, the increase of [Lt]/[DFe] ratios from east to west was caused by both the concentrations of dissolved Fe (decrease) and the ligand concentration (increase). Obviously the excess ligand concentration also increased from east to west in the Weddell Gyre resulting in the increase of organic alpha value and combined with the decrease in the dissolved Fe concentration, an increase in pFe. Finally, the relatively high ratios of [Lt]/[DFe] in the deep part of the Drake Passage were due to high concentrations of ligand (1.31 Eq of nM Fe, n = 6) and remarkably constant excess L with depth.

The ratio [Lt]/[DFe] was constant below 450 m. Hunter and Boyd (2007) suggested that Fe-binding ligands in the deep ocean are refractory humic materials that originate from degradation of organic matter in the surface layer. The degradation would generate ligand functional groups in the deep ocean (Kuma *et al.*, 1996; Chen *et al.*, 2003) where only one dominant group of ligands is present (Rue and Bruland, 1995; Hunter and Boyd, 2007). The ligand characteristics found in the deep ocean in our samples were indeed relatively constant with depth (constant pFe and organic alpha reflecting an equilibrium between ligands, precipitation and adsorption of Fe) or showed a slight vertical trend, with increasing depth a decrease of excess L, and slight increase of K' value (Tables 2 and 3; Figures 2, 3 and 4). The ligand characteristics in the deep ocean reflect either a balance between production and degradation of dissolved organic ligands or a constant very refractory type/group of ligands. If constant production of ligands by microbial activity with depth exists (Reid *et al.*, 1993) it must be balanced by a constant degradation of ligands (Powell and Donat, 2001). Witter and Luther (1998) showed with a kinetic approach a change in the formation rate of Fe-ligand complexes and consequently the change of the dissociation rate (slower in the deep). They suggested that very slow degradation of ligands results in long residence time of the ligands (up to 1000 yr). Our data could

confirm this statement since the southward flowing water is depleted in Fe but not in ligand: Our study showed a uniform concentration of dissolved organic ligand and a rather uniform K' in deep waters, causing constant organic alpha and pFe values, not suggesting transformation of ligand characteristics with time as suggested by Witter and Luther (1998). Since the trend in [Lt]/[DFe] ratio in the deep waters between geographical locations (Figures 1, 3 and 4, Table 3) was a consequence of what happened in the surface layer, the export of particulate organic matter is important. Knowledge of Fe in other size fractions, like the particulate fraction from unfiltered water and different colloidal size fractions would help to understand which processes control the ligands and the Fe distribution in the deep ocean.

6. Conclusions

Overall the observed trends in [Lt]/[DFe] ratio values with depth and geographical location were consistent with the changes in ligand characteristics (excess L, organic alpha and resulting pFe) but showed a much clearer trend than the separate other parameters and confirmed that the ratio [Lt]/[DFe] is a reliable concept to study the chemistry of Fe in the oceans. This study has shown clear differences between upper waters (until 450 m depth), influenced by the presence of the phytoplankton, and deeper waters (below 450 m depth) in dissolved organic ligand characteristics and in the distribution of dissolved Fe. These high ratios (3.7-66.9) at the surface decreased to a nearly constant value below 450 m (1.7-3.6). Both the upper (0-450 m) and deeper (below 450 m) parts of the ocean showed an increasing trend southwards. In the upper 450 m this trend reflected the increasing depletion of Fe resulting in HNLC waters with increasing distance from Fe sources. However, the ligands also showed an increasing trend southwards showing that they are very resistant to degradation. In the upper layer of the Weddell Gyre, the increase in [Lt]/[DFe] ratio values from east to west is due to a decrease in dissolved Fe concentrations. In the deeper waters of the Weddell Gyre it is due to both the increase of ligand and the decrease of dissolved Fe concentrations. In the deep waters (below 450 m depth) a steady state between dissolved organic ligand and dissolved Fe was found at any location reflecting a balance between production and degradation of the organic matter. With the increase

of dissolved Fe concentrations with depth, the ligand sites for binding Fe are getting filled, and even almost saturated (North of the SB on the Zero Meridian). This near-saturation is deemed to be consistent with the precipitation of Fe as insoluble oxyhydroxide and its removal to the deep ocean. It confirms the important role of the organic ligands in keeping Fe in the soluble phase, thus avoiding its precipitation, and increasing its residence time in the water column. In the deeper layer (> 450 m) the increase in the [Lt]/[DFe] ratio is caused by a decrease in dissolved Fe concentrations only. A consistent trend in [Lt]/[DFe] values, at various depths and locations, is in itself impressive since nobody, to our knowledge, ever found clear trends in ligand characteristics other than a general decrease in ligand concentration with depth. However, the explanation is not still completely clear. The competition in the overall Fe budget between stabilisation by organic ligands and the removal by scavenging (adsorption onto particulate matter and colloid aggregation with or without oxidative precipitation) needs to be taken into account in order to better understand the Fe cycle in the ocean.